Effect of polymer morphology on P3HT-based solid-state dye sensitized solar cells: an ultrafast spectroscopic investigation

R. Sai Santosh Kumar,[1,*] G. Grancini,[1,3] A. Petrozza,[1] A. Abrusci,[3] H. J. Snaith,[3] and G. Lanzani[1,2]

[1]Center for Nano Science and Technology @Polimi, Istituto Italiano di Tecnologia, via .Giovanni Pascoli 70/3, 20133 Milano, Italy

[2]*Dipartimento di Fisica, Politecnico di Milano, Piazza L. da Vinci, 32, 20133 Milano, Italy*

[3]*Oxford University, Department of Physics, Clarendon Laboratory, Parks Road, Oxford, OX13PU, UK*

[*]*santosh.raavi@iit.it*

Abstract: Solid-state dye sensitized solar cell devices are fabricated with poly(3-hexylthiophene) (P3HT) as the hole transporting layer. Upon annealing treatment we obtained ≈70% increase in the device efficiency compared to un-annealed devices. Our investigation, by means of ultrafast transient absorption spectroscopic characterization, correlates the increased device performances to a more efficient hole-transfer at the dye/polymer interface in the thermally treated P3HT.

OCIS codes: (350.6050) Solar energy; (160.5470) Polymers; (040.5350) Photovoltaic; (320.7150) Ultrafast spectroscopy.

References and Links

1. A. Yella, H.-W. Lee, H. N. Tsao, C. Yi, A. K. Chandiran, M. K. Nazeeruddin, E. W. Guang Diau, C. Yu Yeh, S. M. Zakeeruddin, and M. Grätzel, "Porphyrin-sensitized solar cells with cobalt (II/III)–based redox electrolyte Exceed 12 percent efficiency," Science **324**, 634–639 (2011).
2. A. Hagfeldt, G. Boschloo, L. Sun, L. Kloo, and H. Pettersson, "Dye-sensitized solar cells," Chem. Rev. **110**(11), 6595–6663 (2010).
3. M. Grätzel, "Photoelectrochemical cells," Nature **414**(6861), 338–344 (2001).
4. H. J. Snaith and L. Schmidt-Mende, "Advances in liquid-electrolyte and solid-State dye-sensitized solar cells," Adv. Mater. **19**(20), 3187–3200 (2007).
5. M. Grätzel, U. Bach, D. Lupo, P. Comte, J. E. Moser, F. Weissörtel, J. Salbeck, and H. Spreitzer, "Solid-state dye-sensitized mesoporous TiO_2 solar cells with high photon-to-electron conversion efficiencies," Nature **395**(6702), 583–585 (1998).
6. J. Burschka, A. Dualeh, F. Kessler, E. Baranoff, N. L. Cevey-Ha, C. Yi, M. K. Nazeeruddin, and M. Grätzel, "Tris(2-(1H-pyrazol-1-yl)pyridine)cobalt(III) as p-type dopant for organic semiconductors and its application in highly efficient solid-state dye-sensitized solar cells," J. Am. Chem. Soc. **133**(45), 18042–18045 (2011).
7. D. Poplavskyy and J. Nelson, "Nondispersive hole transport in amorphous films of methoxy-spirofluorenearylamine organic compounds," J. Appl. Phys. **93**(1), 341–346 (2003).
8. I.-K. Ding, J. Melas-Kyriazi, N.-L. Cevey-Ha, K. G. Chittibabu, S. M. Zakeeruddin, M. Grätzel, and M. D. McGehee, "Deposition of hole-transport materials in solid-state dye-sensitized solar cells by doctor-blading," Org. Electron. **11**(7), 1217–1222 (2010).
9. G. K. Mor, S. Kim, M. Paulose, O. K. Varghese, K. Shankar, J. Basham, and C. A. Grimes, "Visible to near-infrared light harvesting in TiO_2 nanotube array-P3HT based heterojunction solar cells," Nano Lett. **9**(12), 4250–4257 (2009).
10. R. Zhu, C. Y. Jiang, B. Liu, and S. Ramakrishna, "Highly efficient nanoporous TiO_2-polythiophene hybrid solar cells based on interfacial modification using a metal-free organic dye," Adv. Mater. **21**(9), 994–1000 (2009).
11. A. Abrusci, R. S. S. Kumar, M. Al-Hashimi, M. Heeney, A. Petrozza, and H. J. Snaith, "Influence of ion induced local coulomb field and polarity on charge generation and efficiency in poly (3-Hexylthiophene) -based solid-state dye-sensitized solar cells," Adv. Funct. Mater. **21**(13), 2571–2579 (2011).
12. W. Zhang, Y. Cheng, X. Yin, and B. Liu, "Solid-State Dye-Sensitized Solar Cells with Conjugated polymers as Hole-Transporting Materials," Macromol. Chem. Phys. **212**(1), 15–23 (2011).
13. L. Yang, U. B. Cappel, E. L. Unger, M. Karlsson, K. M. Karlsson, E. Gabrielsson, L. Sun, G. Boschloo, A. Hagfeldt, and E. M. J. Johansson, "Comparing spiro-OMeTAD and P3HT hole conductors in efficient solid state dye-sensitized solar cells," Phys. Chem. Chem. Phys. **14**(2), 779–789 (2011).

#185264 - $15.00 USD Received 12 Feb 2013; revised 24 Mar 2013; accepted 27 Mar 2013; published 22 Apr 2013

14. G. Grancini, R. S. S. Kumar, M. Maiuri, J. Fang, W. T. S. Huck, M. Alcocer, G. Lanzani, A. Petrozza, G. Cerullo, and H. J. Snaith, "Panchromatic "dye-doped" polymer solar cells: from femtosecond energy relays to enhanced photo-response," J. Chem Phys. Lett. **4**(3), 442–447 (2013).
15. J. Cabanillas-Gonzalez, G. Grancini, and G. Lanzani, "Pump-probe spectroscopy in organic semiconductors: monitoring fundamental processes of relevance in optoelectronics," Adv. Mater. **23**(46), 5468–5485 (2011).
16. R. S. S. Kumar, L. Lüer, D. Polli, M. Garbugli, and G. Lanzani, "Primary photo-events in a metastable photomerocyanine," Opt. Mater. Express **1**(2), 293–304 (2011).
17. I. A. Howard and F. Laquai, "Optical probes of charge generation and recombination in bulk heterojunction organic solar cells," Macromol. Chem. Phys. **211**(19), 2063–2070 (2010).
18. G. Grancini, R. S. Santosh Kumar, A. Abrusci, H.-L. Yip, C.-Z. Li, A.-K. Y. Jen, G. Lanzani, and H. J. Snaith, "Boosting infrared light harvesting by molecular functionalization of metal oxide/polymer interfaces in efficient hybrid solar cells," Adv. Funct. Mater. **22**(10), 2160–2166 (2012).
19. A. Listorti, B. O'Regan, and J. R. Durrant, "Electron transfer dynamics in dye-sensitized solar cells," Chem. Mater. **23**(15), 3381–3399 (2011).
20. M. D. Brown, T. Suteewong, R. S. S. Kumar, V. D'Innocenzo, A. Petrozza, M. M. Lee, U. Wiesner, and H. J. Snaith, "Plasmonic dye-sensitized solar cells using core-shell metal-insulator nanoparticles," Nano Lett. **11**(2), 438–445 (2011).
21. T. Horiuchi, H. Miura, and S. Uchida, "Highly efficient metal-free organic dyes for dye-sensitized solar cells," J. Photochem. Photobiol. A **164**(1-3), 29–32 (2004).
22. H. Snaith, "How should you measure your excitonic solar cells?" Energy Environ. Sci. **5**(4), 6513–6520 (2012).
23. R. Jose, A. Kumar, V. Thavasi, and S. Ramakrishna, "Conversion efficiency versus sensitizer for electrospun TiO_2 nanorod electrodes in dye-sensitized solar cells," Nanotechnology **19**(42), 424004 (2008).
24. X. M. Jiang, R. Österbacka, O. Korovyanko, C. P. An, B. Horovitz, R. A. J. Janssen, and Z. V. Vardeny, "Spectroscopic studies of photoexcitations in regioregular and regiorandom polythiophene films," Adv. Funct. Mater. **12**(9), 587–597 (2002).
25. R. A. Marsh, J. M. Hodgkiss, S. Albert-Seifried, and R. H. Friend, "Effect of annealing on P3HT:PCBM charge transfer and nanoscale morphology probed by ultrafast spectroscopy," Nano Lett. **10**(3), 923–930 (2010).
26. J. Kirkpatrick, P. E. Keivanidis, A. Bruno, F. Ma, S. A. Haque, A. Yarstev, V. Sundstrom, and J. Nelson, "Ultrafast transient optical studies of charge pair generation and recombination in poly-3-hexylthiophene(P3ht):[6,6]phenyl C_{61} butyric methyl acid ester (PCBM) blend films," J. Phys. Chem. B **115**(51), 15174–15180 (2011).
27. V. D. Mihailetchi, H. Xie, B. de Boer, L. J. A. Koster, and P. W. M. Blom, "Charge transport and photocurrent generation in poly(3-hexylthiophene):methanofullerene bulk-heterojunction solar cells," Adv. Funct. Mater. **16**(5), 699–708 (2006).
28. C. Goh, S. R. Scully, and M. D. McGehee, "Effects of molecular interface modification in hybrid organic-inorganic photovoltaic cells," J. Appl. Phys. **101**(11), 114503 (2007).
29. Y. Kim, S. Cook, S. M. Tuladhar, S. A. Choulis, J. Nelson, J. R. Durrant, D. D. C. Bradley, M. Giles, I. McCulloch, C.-S. Ha, and M. Ree, "A strong regioregularity effect in self-organizing conjugated polymer films and high-efficiency polythiophene:fullerene solar cells," Nat. Mater. **5**(3), 197–203 (2006).
30. W. H. Howie, F. Claeyssens, H. Miura, and L. M. Peter, "Characterization of solid-state dye-sensitized solar cells utilizing high absorption coefficient metal-free organic dyes," J. Am. Chem. Soc. **130**(4), 1367–1375 (2008).
31. E. V. Canesi, M. Binda, A. Abate, S. Guarnera, L. Moretti, V. D'Innocenzo, R. S. S. Kumar, C. Bertarelli, A. Abrusci, H. Snaith, A. Calloni, A. Brambilla, F. Ciccacci, S. Aghion, F. Moia, R. Ferragut, C. Melis, G. Malloci, A. Mattoni, G. Lanzani, and A. Petrozza, "The effect of selective interactions at the interface of polymer–oxide hybrid solar cells," Energy Environ. Sci. **5**(10), 9068–9076 (2012).
32. W. C. Tsoi, S. J. Spencer, L. Yang, A. M. Ballantyne, P. G. Nicholson, A. Turnbull, A. G. Shard, C. E. Murphy, D. D. C. Bradley, J. Nelson, and J.-S. Kim, "Effect of crystallization on the electronic energy levels and thin film morphology of P3HT:PCBM Blends," Macromolecules **44**(8), 2944–2952 (2011).

1. Introduction

Solid-state dye-sensitized solar cells (sDSC) are a potential alternative to liquid electrolyte based conventional DSCs as they promise to circumvent stability issues of DSC caused by several effects such as the evaporation and leakage of liquid and the corrosion of counter-electrode [1–4], in addition to being easier to manufacture. As solid state hole transporter material (HTM) the most successfully employed is 2,2',7,7'-tetrakis(N,N-di-4-methoxyphenylamino)-9,9'-spirobifluorene (spiro-OMeTAD) [5] with a demonstrated power conversion efficiency (PCE) of 7.2% [6]. Although spiro-OMeTAD is among the first and longest standing organic HTM for sDSCs, it has some disadvantages such as low hole-mobility ($\approx 10^{-4} cm^2 V^{-1} sec^{-1}$) [4,7] and relatively complex multistage synthesis [8]. Consequently, there is now a hot pursuit on the utility of conjugated polymers (CPs) as

#185264 - $15.00 USD Received 12 Feb 2013; revised 24 Mar 2013; accepted 27 Mar 2013; published 22 Apr 2013

alternative HTMs due to their thermal stability, high conductivity, good solubility as well as tunable optoelectronic properties [9–13]. Additionally, they can also be used as cooperative light antenna to achieve panchromatic absorption in very thin films [14]. We employ the ubiquitous semiconducting polymer in organic solar cells, poly(3-hexylthiophene) (P3HT), as the hole transport material for sDSC [13].

In this work, we address the relationship between the morphological properties of P3HT and the charge generation/recombination dynamics, ultimately related to the device efficiency. We show that upon thermal annealing, which is well known to induce the formation of more crystalline P3HT phases, the device efficiency increases by ≈70% and the short circuit current density (J_{sc}) increases of about ≈80%. To obtain insight into the charge generation mechanism at the polymer/dye interface, we employ femtosecond transient absorption spectroscopy (TAS) [15, 16] as a powerful tool to obtain fundamental knowledge on the photophysical properties and dynamical processes in photovoltaics system [17–20]. The results of our photophysical investigation show that the improved crystallinity of the P3HT induces a more efficient hole-transfer from the organic dye to the polymer and reduces charge recombination, having a direct impact on the observed improvement on the device performances.

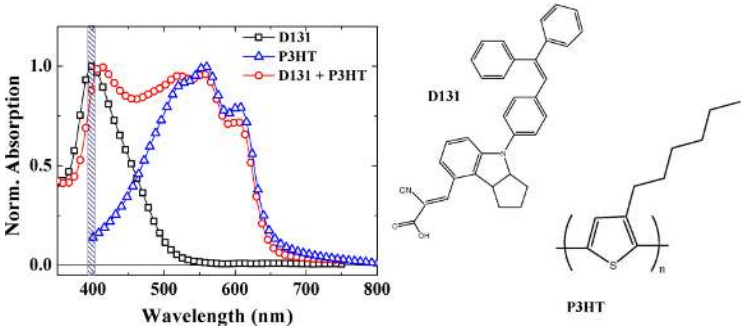

Fig. 1. Normalized absorption spectra and molecular structure of D131, P3HT and the complete photovoltaic composite deposited on 1 µm TiO_2. The shaded region represents the excitation pulse used for fs-TAS.

2. Experimental details

The devices are fabricated using the procedure followed in our earlier work for optimized performances including the use of additives Li-TFSI and *t*BP [11]. The dye chosen for this work is the organic dye termed D131 [21] sensitized on 1µm thick mesoporous TiO_2. We fabricated devices with region-random (RRa) and region-regular (RRe) P3HT as hole-transporter. We annealed the devices for 20 minutes at temperature of 140 °C. The current-voltage characteristics of all the devices under AM1.5 simulated sun light of 100 $mWcm^{-2}$ have been measured using round metal mask to reduce the light piping [22]. To obtain repeatability 40 devices were fabricated and tested. During testing the active areas of the devices were defined by single aperture metal optical masks with a round aperture of 2.5 mm giving an area of 0.0491 cm^2. We note that all light was excluded from entering the sides of the devices by having them in a "light-tight" sample holder, and the only light entering the solar cell substrate was through the single mask aperture. For the fs-TAS experiment, the laser source is an amplified mode locked Ti:sapphire laser (Clark-MXR Model CPA-1), delivering pulses at 1kHz repetition rate with 780 nm center wavelength, 150 fs duration. In the present work we used the second harmonic of fundamental centered at 390 nm as a pump pulse to excite the sample. Another small fraction of the Ti: sapphire amplified output is independently focused into a 1-mm-thick sapphire plate to generate a stable single-filament white-light supercontinuum which serves as a probe pulse. In a typical pump-probe experiment, the system under study is resonantly photoexcited by a short "pump" pulse and

#185264 - $15.00 USD Received 12 Feb 2013; revised 24 Mar 2013; accepted 27 Mar 2013; published 22 Apr 2013

its subsequent dynamical evolution is detected by measuring the transmission (T) changes of a delayed "probe" pulse as a function of pump-probe delay τ given by the differential transmission $\Delta T/T[= (T_{pump\text{-}on}\text{-}T_{pump\text{-}off})/T_{pump\text{-}off}$]. The pump and probe beams are spatially and temporally overlapped on the sample, controlling the time delay by a motorized slit. The minimum detectable signal is $\Delta T/T \approx 10^{-4}$ and the instrument response obtained is ≈200 fs time. The pump beam energy density used in the experiment is kept deliberately low (pump fluence = 10 μJ/cm^2) to minimize bimolecular effects. All the measurements were taken with the samples in a vacuum chamber, to prevent any influence from oxygen or sample degradation.

3. Results and discussion

Figure 1(a) shows the absorption spectrum of the D131 sensitized TiO_2 with (red circles) and without (black squares) RRe-P3HT. The dye shows a major absorption peak at 400 nm. Evidently the absorption spectra of P3HT (blue triangle) is complementary to the D131 absorption spectrum. From earlier reports, the HOMO levels of P3HT and D131 are assumed to be −5.10 eV [10] and −5.017 eV [23] respectively, relative to vacuum. This energetic-landscape would favor hole-transfer from dye to P3HT making it a suitable candidate as a hole transporting layer. The design of the sDSC fabricated for the experiment is shown in Fig. 2(a). The polymer is deposited on the D131-sensitized TiO_2 mesoporous structure. The polymer infiltrates into the metal oxide pores and leaves a capping layer about of 200 nm thick. As a first attempt, we fabricated devices using regio-regular (RRe) P3HT and regio-random (RRa) P3HT. As seen from Fig. 2(b) devices with RRe-P3HT show better efficiency of 1.7% compared to 0.54% obtained with the RRa- P3HT. The photo-current density versus voltage traces for the sDSC were measured under AM 1.5G simulated sun light.

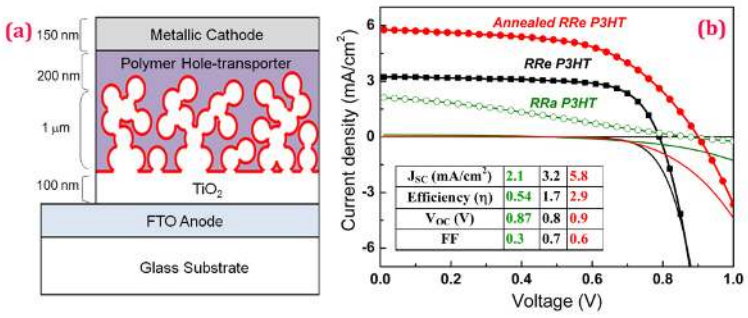

Fig. 2. (a) Schematic design of the fabricated sDSC; (b) J-V characteristic for RRa P3HT (green empty dots), RRe P3HT (black full squares), thermal annealed RRe P3HT (red dotted line) and corresponding dark current in solid line. In the inset the table showing the device parameters

As a step forward, we annealed the RRe-P3HT devices at 140 °C for 20 minutes, before evaporating the top contact electrodes. The results (see dotted line in Fig. 2b) show an improved efficiency of 2.9%, leading to an increase of ≈70% compared to the un-annealed device. Significantly, J_{sc} increases from 3.2 mA/cm^2 to 5.8 mA/cm^2 upon thermal treatement suggesting an increase of ≈80% in the overall photo-generated charges reaching the electrodes upon annealing. No change in device performance is observed while annealing RRa-P3HT, suggesting annealing has no direct effect on it. The RRe-P3HT is known to have a planar backbone with respect to the twisted RRa-P3HT geometry (with inherent amorphous nature), leading to a higher crystallinity of the thin film, effect that is even more amplified upon annealing. This definitely affects the optoelectronic properties of the material [24–29]. For example, in P3HT: PCBM blend the hole-mobility in the P3HT phase is known to

#185264 - $15.00 USD Received 12 Feb 2013; revised 24 Mar 2013; accepted 27 Mar 2013; published 22 Apr 2013

increase by more than three orders of magnitude upon annealing [27]. Therefore, upon annealing we conjecture improved device performances owing to change in morphology of the P3HT film itself. Additionally, we observe that open-circuit voltage (V_{OC}) has slightly higher value upon annealing which can be surmised due to reduced charge-recombination pathways because of a different local morphology in the polymer for the annealed device. Also, contrary to our expectations we notice that the fill-factor (FF) obtained for the annealed device, though in agreement with data reported in literature [10, 11], has a slight reduction upon annealing. To this, we conjecture that the presence of additives might have an impact [2,10,11]. In particular, together with the different local morphology induced by annealing they can affect the charge dynamics thus resulting in minor variation of the FF. However, further investigations are needed to better address the variation in V_{OC} and FF upon annealing.

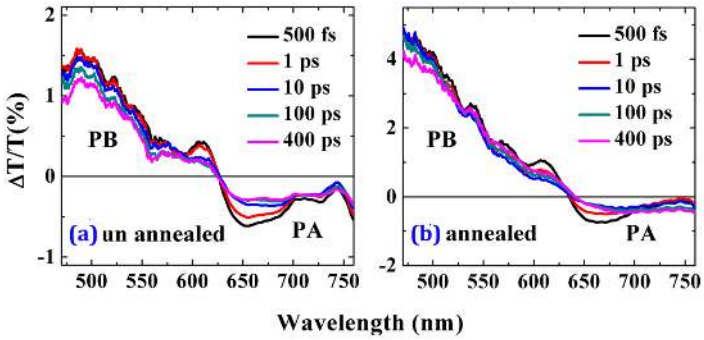

Fig. 3. ΔT/T spectra of TiO_2/D131/P3HT (a) un-annealed and (b) annealed devices by exciting the dye molecules at 390nm and probe in both the VIS spectral region.

In order to get insights on the effect of the nano-morphology on the photoexcited species and on their dynamics, we performed fs-TAS directly on samples which preserve the device configuration (without the top electrodes) before and after annealing. We tune the photoexcitation to 390 nm to predominantly excite the dye only. Upon photo-excitation, at the dye/TiO_2 interface the exciton formed in the D131 dissociates and electrons are effectively injected into the metal oxide. Generally, the electron injection from an organic dye to TiO_2 starts within the first 500 fs of the photo-excitation [11]. After the electron is injected, the hole is left in the dye, thus creating the oxidized dye species $D131^+$ [30]. We identified the PA of $D131^+$ species in the spectral region of 550-650 nm by performing the fs-TAS measurements of D131 adsorbed on TiO_2 before depositing P3HT layer. In the device configuration after the deposition of P3HT as shown in Fig. 2(a) the dye is interfaced with P3HT. Due to the favorable HOMO level alignment of D131 and P3HT, the hole in D131 should transfer to P3HT thus forming $P3HT^+$. Figure 3 shows the ΔT/T spectra of (a) un-annealed and (b) annealed samples. We can distinguish a positive band at shorter wavelength side of the spectrum that corresponds to the dye photobleaching (PB), in fair agreement with the ground-state absorption of the overall device material components. Though at 390 nm the dye molecules are resonantly excited, it should be noted that also P3HT partially absorbs at 390 nm (see Fig. 1) and hence the observation of a PB spectral band at 600 nm. In particular, we expect a contribution of the disordered P3HT phase for wavelengths shorter than 550nm. We assign the photo-induced absorption (PA) bands PA to $D131^+$ partially overlapping with PA of $P3HT^+$ species [31] peaking at 750 nm.

Investigating further into the kinetics of probe wavelengths at, 610 nm and 730 nm as shown in Fig. 4 we obtained important conclusions. From the absorption spectra of D131 (see Fig. 1) we expect a dominant contribution from the dye molecules to the PB till 500 nm. The probe wavelength at 610 nm represents the 0–0 transition of P3HT [25] and the kinetics at

#185264 - $15.00 USD Received 12 Feb 2013; revised 24 Mar 2013; accepted 27 Mar 2013; published 22 Apr 2013

610 nm corresponds to the PB of P3HT. As shown in Fig. 4(a) for the un-annealed devices we observe that the PB due to the partial photoexcitation of P3HT shows a sharp initial decay in the first 2 ps followed by a slower decay in the hundreds of ps timescale. The initial fast component has been assigned to the geminate recombination of charge pairs instantaneously formed in the P3HT [24]. The following slow decay kinetics, we conjecture, is related to the residual $P3HT^+$ species after hole-transfer from the oxidized D131 to the P3HT occurs. Correspondingly, as shown in Fig. 4(b), we observe the charge recombination kinetics of the $P3HT^+$ species at 730 nm (PA_1) follow similar trend for un-annealed devices. The kinetics of annealed films at 610 nm and 730 nm, till probe delay of 2 ps, the kinetics follow similar trend as observed in the un-annealed devices. The scenario changes completely after 2 ps, for instead of the slow-decay kinetics we observe a rapid monotonous growth of the PB at 610 nm that matches the growth in the PA_1 band at 730 nm till the end of our temporal probe-delay window of 400 ps. We assign this growth to an increased population of $P3HT^+$ charges due to an increase in efficiency of hole-transfer occurring at the dye/P3HT interfaces. The rise of the $P3HT^+$ species reduces the ground state population of P3HT inducing an increase of the PB at 610 nm as well as the growth of $P3HT^+$ absorbing species at 730 nm. This enhanced hole-transfer and rise in the overall $P3HT^+$ species upon annealing can also be due to the shift in the P3HT HOMO level upon crystallization [32] that can induce a larger driving force for hole-transfer at the interface. Additionally, enhanced hole-mobility due to better ordering in the annealed polymer [27] induces a faster charge transport in the P3HT layer away from the dye/P3HT interface, potentially reducing recombination between electrons trapped at the dye-TiO_2 interface with the holes on the P3HT. From these investigations we can conclude that annealing the device enables a better hole-transfer at the dye/ P3HT interface.

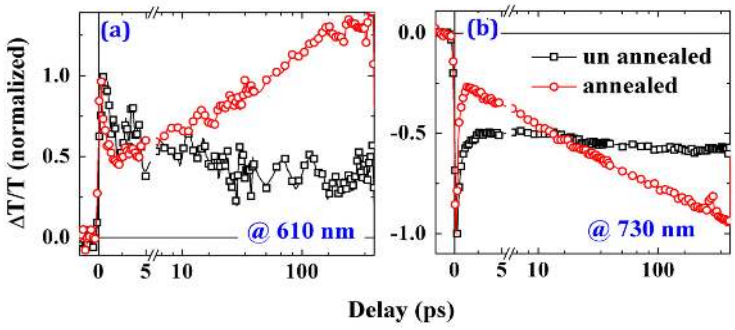

Fig. 4. Comparison of ΔT/T dynamics at: (a) 610nm, (b) 730nm for un-annealed (black -□-) and annealed (red –o-) devices.

4. Conclusions

We performed a systematic investigation on the effect of the polymer morphology of the P3HT used as hole-transport layer in solid-state dye sensitized solar cells (sDSC). Fabricated devices are tested before and after annealing and were observed to show ≈80% increase in J_{sc} and ≈70% in efficiency after annealing. We performed fs-TAS experiments to investigate the effect of morphology on the hole-transfer and recombination dynamics. We observed that upon annealing there is enhancement in the hole-transfer from dye to P3HT along with enhanced hole-mobility, thus being an effective way to increase the overall device performances.

Acknowledgments

Authors thank Mr. Andy Hey, University of Oxford, for his contribution to the illustration. We thank EPSRC for funding, and the Royal Society International Exchange Scheme 2012/R2 for supporting this collaboration.

#185264 - $15.00 USD Received 12 Feb 2013; revised 24 Mar 2013; accepted 27 Mar 2013; published 22 Apr 2013